Low-frequency conductivity of a nondegenerate two-dimensional electron liquid in strong magnetic fields

M. I. Dykman*

*Department of Physics and Astronomy and Institute for Quantum Sciences, Michigan State University,
East Lansing, Michigan 48824, USA*

Leonid P. Pryadko[†]

Department of Physics, University of California, Riverside, California 92521, USA

We study the conductivity of a nondegenerate two-dimensional electron liquid in a quantizing magnetic field for frequencies well below the cyclotron frequency. The conductivity is formed by electron transitions in which the energy of a photon goes to the interaction energy of the many-electron system, whereas the involved momentum is transferred to the quenched disorder. The conductivity peak is non-Lorentzian. Its shape depends on the relation between the correlation length r_c of the disorder potential and the typical amplitude δ_f of vibrations of the electrons about their quasiequilibrium positions in the liquid. The width of the peak is determined by the reciprocal time it takes to move an electron over r_c (or the magnetic length l for $r_c < l$). In turn, this time is determined by vibrational or diffusive motion, depending on the ratio r_c/δ_f. We analyze the tail of the conductivity peak for a short-range disorder. It is formed by multiple collisions with the disorder potential. We also analyze scattering by rare negatively charged traps, and show that the conductivity spectrum in this case depends on both short- and long-time electron dynamics.

I. INTRODUCTION

In recent years, much progress has been made toward the understanding of transport phenomena in strongly interacting electron systems. The well-known examples are the fractional quantum Hall effect[1] (QHE) and metal-insulator transition phenomena in low-density two-dimensional electron systems (2DESs) in semiconductors.[2] 2DESs are particularly convenient for investigating the electron-electron interaction (EEI), since the electron density n can be varied in broad limits. One of the most important effects of the EEI is the onset of electron correlations. The extent to which the system is correlated depends on the ratio Γ of the characteristic Coulomb energy $e^2(\pi n)^{1/2}$ to the electron kinetic energy E_{kin},

$$\Gamma = e^2(\pi n)^{1/2}/E_{kin} \qquad (1)$$

(E_{kin} is equal to the largest of the Fermi energy ϵ_F and $k_B T$). For Γ exceeding a critical value Γ_W, a 2DES becomes a Wigner crystal. The parameter Γ_W is numerically large. For low temperatures ($E_{kin} = \epsilon_F \gg k_B T$, in which case $\Gamma = r_s$), $\Gamma_W \approx 37$,[3] whereas for a nondegenerate 2DES ($\epsilon_F \ll k_B T$) $\Gamma_W \approx 130$.[4]

For $\Gamma_W > \Gamma \gg 1$, a 2DES is still strongly correlated, but it forms an electron liquid. Based on the success of the Fermi-liquid theory in describing ^{3}He, it is often assumed that in the quantum region $\epsilon_F \gg k_B T$, the electron liquid can be described by a Fermi liquid, too. However, for very large r_s, the system may be more complex.[3,5]

For large $k_B T/\epsilon_F$ and for $\Gamma_W > \Gamma \gg 1$, a 2DES is a strongly correlated non-Fermi liquid. It should display a nonstandard behavior. Experimentally, such a 2DES has been investigated in semiconductor heterostructures,[2,6] and in much detail for electrons on the surface of liquid helium.[4] A nondegenerate electron liquid has features in common with an ordinary liquid. It does not have a long-range translational order and displays self-diffusion, as seen in various numerical simulations.[7–10]

In contrast to ordinary liquids driven by forces applied to their surface, a 2DES is driven by a "volume" field, that is, a field experienced by each electron. It comes from the external disorder, such as defects and phonons in semiconductors, or helium vapor atoms and surface capillary waves on helium. Because the total momentum of a 2D electron liquid is changed through volume rather than "surface" scattering, electron transport is different from transport in an ordinary liquid. It is different also from the transport in a weakly nonideal electron gas. Even though the conductivity is of a metallic type rather than the activated type for a weak disorder potential, its dependence on the parameters of the system, including electron density, temperature, frequency, and a magnetic field, should be totally different from that for an ideal gas.

The change of transport coefficients stems from the electron scattering by disorder being strongly affected by the electron-electron interaction in a 2D liquid. During scattering, an electron is coupled to other electrons, and this coupling determines the scattering probability. This is the case even for a short-range disorder potential, where different electrons are scattered off uncorrelated fluctuations. In this respect, a nondegenerate electron liquid is similar to a liquid of vortices in a superconductor.

In the present paper, we investigate the frequency dependence of the magnetoconductivity $\sigma_{xx}(\omega)$ of a 2D electron liquid. Such a dependence is particularly interesting, since it should provide a direct insight into the way in which a correlated electron system exchanges momentum with the dis-

order. Indeed, in the Drude model the low-frequency magnetoconductivity, transverse to a strong magnetic field B, is

$$\sigma_{\mathrm{Dr}}(\omega) = ne^2 \tau_{\mathrm{Dr}}^{-1}(\omega)/m\omega_c^2, \quad \omega_c = eB/mc, \quad (2)$$

where ω_c is the cyclotron frequency and τ_{Dr}^{-1} is the momentum relaxation rate. Here and below, we keep in $\sigma_{xx}(\omega)$ the lowest-order term in ω_c^{-1}. The frequency dispersion of σ_{Dr} comes from the dispersion of $\tau_{\mathrm{Dr}}^{-1}(\omega)$. In the case of single-electron elastic scattering, it becomes strong for frequencies of the order of the duration of a collision with a scatterer.

The single-electron Drude picture does not apply to a 2DES if the magnetic field B transverse to the electron layer is quantizing. Here, all single-electron states except for one or maybe few are localized,[11,12] and the single-electron conductivity is equal to zero at zero frequency.[13,14] Metalliclike conductivity of a nondegenerate electron liquid is a result of the electron-electron interaction. Earlier, we found a way to take this interaction into account nonperturbatively, and calculated the static conductivity and the cyclotron resonance for a weak short-range disorder potential.[15] These results were qualitatively and quantitatively confirmed by the experiment.[16,17]

The question of observing the actual dynamics or electron scattering in the electron liquid has not been addressed previously. From analogy with single-electron scattering one may expect that an insight into this dynamics can be gained from the frequency dependence of $\sigma_{xx}(\omega)$. Here, we develop an appropriate theory and suggest relevant experiments. We also study the magnetoconductivity for two important types of a disorder potential, which have not been discussed for a nondegenerate electron liquid: a smooth random potential and a potential of rare charged defects. The physics of many-electron transport in these cases is significantly different from that for short-range disorder.

A simple argument shows that the frequency dispersion of the long-wavelength magnetoconductivity for $\omega \ll \omega_c$ is indeed directly related to many-electron effects. Because the electron kinetic energy is quantized, the energy of an absorbed photon, $\hbar\omega$, may go to either the electron potential energy in the disorder potential or the Coulomb energy of the electron system, or both. For a weak disorder, electrons are not localized, and the disorder potential is largely averaged out by electron motion. Then, the photon energy may only be transferred to the electron system. However, to provide momentum conservation, this transfer must be mediated by disorder.

For a short-range disorder, one can think of photon absorption as resulting from an electron bouncing off a point defect. In a quantizing magnetic field $\mathbf{B}$, momentum transfer to defect $\delta\mathbf{p}$ leads to an electron displacement $\delta\mathbf{r} = (c/eB^2)\,\delta\mathbf{p} \times \mathbf{B}$. In the presence of radiation, this displacement can change the energy of the electron-electron interaction by $\hbar\omega$. Therefore, by investigating the frequency dependence of the absorption cross section, one can find how an electron moves during a collision.

As we show, for a weak short-range disorder the conductivity $\sigma_{xx}(\omega)$ has a peak at $\omega = 0$ with a specific non-Lorentzian shape, which is fully determined by the electron-

electron interaction. Of special interest is the tail of this peak. For large photon frequencies (but still $\omega \ll \omega_c$), a large electron displacement $\delta\mathbf{r}$ is required in order to accommodate the energy. Consequently, a large momentum has to be transferred to the disorder potential. It may come from multiple scattering off this potential. The mechanism has some similarity with that of anomalous diffusion transverse to a magnetic field.[18] It significantly slows down the decay of $\sigma_{xx}(\omega)$, with ω compared to the decay calculated for a single-collision absorption.

The frequency dependence of $\sigma_{xx}(\omega)$ is totally different for a long-range disorder potential. Of particular interest is the potential with a correlation length r_c smaller than the interelectron distance. In this case, the electron scattering cannot be described in the hydrodynamic approximation. As we show, here the conductivity displays a characteristic cusp at $\omega = 0$.

In Sec. II, we relate the magnetoconductivity of a strongly correlated electron liquid to the electron structure factor. We introduce the single-site approximation, which determines the short-wavelength behavior of the structure factor. In Sec. III, we analyze the frequency dependence of the magnetoconductivity for a short-range disorder potential. We show that, for nonzero frequencies but $\omega \ll \omega_c$, the conductivity in quantizing fields becomes a nonmonotonic function of B. In Sec. IV, we develop an appropriate diagrammatic technique and study the far frequency tail of the magnetoconductivity due to multiple electron scattering. In Sec. V, we discuss two types of an intermediate-range disorder: the smooth disorder potential and the potential of short-range electron traps; in both cases the conductivity is shown to be related to diffusion in the electron liquid. Section VI contains concluding remarks.

II. MANY-ELECTRON MAGNETOCONDUCTIVITY: GENERAL ARGUMENTS

In the range $\Gamma \gg 1$, the energy of the EEI,

$$H_{ee} = \frac{e^2}{2} \sum_{n \neq m} |\mathbf{r}_n - \mathbf{r}_m|^{-1} \quad (3)$$

is the largest in the electron system. Therefore, even where electrons do not form a crystal, $\Gamma < \Gamma_W$, electron positions $\mathbf{r}_n$ are still correlated. The EEI does not change the total momentum of the 2DES, and thus does not directly affect the long-wavelength conductivity $\sigma_{xx}(\omega)$ (the Kohn theorem). However, momentum transfer from electrons to defects depends on electron motion, and so $\sigma_{xx}(\omega)$ is ultimately determined by the EEI.

A standard approach to calculating σ_{xx} is based on finding elementary excitations in the many-electron system and then studying their scattering by a disorder potential. This approach is not of much help in the case of a nondegenerate electron liquid, because elementary excitations are not known.[19] However, for the types of disorder that we are interested in, the frequency-dependent conductivity is determined by electron motion on either short or long times. This motion can be described even when elementary excitations are not known, as explained in the Appendix.

We will consider magnetoconductivity in a quantizing magnetic field B applied normal to the electron layer, $\exp(\hbar\omega_c/k_BT)\gg 1$. Then, the electron wave function is a wave packet. Its typical size is the magnetic length $l=(\hbar/m\omega_c)^{1/2}$. Further analysis is based on the observation[15] that, in addition to a magnetic field, an electron is driven by an electric field $\mathbf{E}_f$ from other electrons. This field is due to electron-density fluctuations, see the Appendix. It leads to a semiclassical drift of the electron wave packet with a group velocity cE_f/B.

The semiclassical approximation applies at sufficiently high temperatures,

$$k_BT\gg\hbar\Omega,\quad \Omega=\omega_p^2/\omega_c\equiv 2\pi e^2n^{3/2}/m\omega_c. \tag{4}$$

Here, Ω is the typical frequency of vibrations of the electrons about their quasiequilibrium positions in the electron liquid (ω_p is the plasma frequency for $B=0$, $\Omega\ll\omega_c$). The picture of moving wave packets, with continuous energy spectrum, is qualitatively different from the single-electron picture where the electron energy spectrum is a set of discrete degenerate Landau levels.

Electron motion leads to the averaging of the disorder potential. Together with interelectron energy exchange it eliminates single-electron localization by an arbitrarily weak random potential studied in the QHE theory.[11,12] A typical electron energy in the liquid is k_BT. Therefore, a sufficiently strong disorder is needed in order to localize an appreciable portion of electrons, potentially leading to a glass transition. In this paper, we assume that the disorder potential is weak and the electron liquid displays self-diffusion and associated self-averaging. Specific conditions depend on the correlation length of the disorder potential and will be discussed later.

A. Magnetoconductivity for a weak disorder potential

The Hamiltonian of the electron liquid in the presence of disorder has the form

$$H=H_0+H_{ee}+H_i,$$

$$H_i=\sum_{\mathbf{q}}V_{\mathbf{q}}\rho_{\mathbf{q}},\quad \rho_{\mathbf{q}}=\sum_n\exp(i\mathbf{q}\cdot\mathbf{r}_n). \tag{5}$$

Here, H_0 is the sum of the single-particle Hamiltonians $p_n^2/2m$ [with $\mathbf{p}_n=-i\hbar\boldsymbol{\nabla}_n+(e/c)\mathbf{A}(\mathbf{r}_n)$]; H_{ee} is the EEI Hamiltonian and is given by Eq. (3), and $V_{\mathbf{q}}$ are the Fourier components of the disorder potential.

The long-wavelength magnetoconductivity is given by the correlator of the total electron momentum $\mathbf{P}=\Sigma\mathbf{p}_n$. The latter satisfies the equation of motion

$$\frac{dP_\mu}{dt}=\omega_c\epsilon_{\mu\nu}P_\nu-i\sum_{\mathbf{q}}q_\mu V_{\mathbf{q}}\rho_{\mathbf{q}}$$

($\epsilon_{\mu\nu}$ is the antisymmetric permutation tensor). The low-frequency conductivity, $\omega\ll\omega_c$, is determined by slow time variation of $\mathbf{P}$. Therefore, the time derivative in this equation can be ignored. The expression for $\mathbf{P}$ can be then substituted

into the Kubo formula for the conductivity, giving $\sigma_{xx}(\omega)$ in terms of the correlator of the density operators $\rho_{\mathbf{q}}$ weighted with the disorder potential,

$$\sigma_{xx}(\omega)=-\frac{e^2l^4[1-\exp(-\beta\omega)]}{4\hbar^3\omega S}\int_{-\infty}^{\infty}dt e^{i\omega t}\sum_{\mathbf{q},\mathbf{q}'}(\mathbf{q}\cdot\mathbf{q}')$$

$$\times\langle V_{\mathbf{q}}V_{\mathbf{q}'}\rho_{\mathbf{q}}(t)\rho_{\mathbf{q}'}(0)\rangle. \tag{6}$$

Here, $\langle\cdots\rangle$ implies thermal averaging followed by averaging over realizations of the random potential, S is the area of the system, and $\beta=\hbar/k_BT$.

In the case of a weak disorder potential, the density-density correlator in Eq. (6) can be evaluated to the zeroth order in $V_{\mathbf{q}}$ (the criteria are discussed below). Then, the conductivity can be expressed in terms of the dynamical structure factor of the electron liquid,

$$S(\mathbf{q},\omega)=\int_{-\infty}^{\infty}dt e^{i\omega t}\tilde{S}(\mathbf{q},t),$$

$$\tilde{S}(\mathbf{q},t)=N^{-1}\langle\rho_{\mathbf{q}}(t)\rho_{-\mathbf{q}}(0)\rangle_0, \tag{7}$$

where $N=nS$ is the total number of electrons, and the subscript 0 means that the correlator is evaluated in the absence of disorder.

For a nondegenerate liquid, it is convenient to write conductivity (6) in the form of an Einstein-type relation

$$\sigma_{xx}(\omega)=\frac{ne^2D_s}{k_BT},\quad D_s=l^2\tau^{-1}(\omega)/4. \tag{8}$$

Here, D_s can be thought of as a coefficient of electron diffusion in the disorder potential; it should not be confused with the coefficient of self-diffusion in the electron liquid discussed in the Appendix. The characteristic diffusion length in the disorder potential is given by the size of the electron wave packet l, and the collision rate is

$$\tau^{-1}(\omega)=\frac{1-e^{-\beta\omega}}{\beta\omega}\hbar^{-2}l^2\sum_{\mathbf{q}}q^2\overline{|V_{\mathbf{q}}|^2}S(q,\omega), \tag{9}$$

where the overline denotes averaging over realizations of disorder.

The rate τ^{-1} (9) is quadratic in the disorder potential, as in the standard Drude approximation. The expression for the conductivity, Eqs. (8) and (9), goes over into the Drude formula (2), if one sets $\tau^{-1}=4\tau_{\mathrm{Dr}}^{-1}/\beta\omega_c$. However, in contrast to the single-electron Drude approximation, the dynamic structure factor in τ^{-1} is determined by the electron-electron interaction. In particular, $S(\mathbf{q},\omega)$ depends on the electron density n.

The factor $[1-\exp(-\beta\omega)]/\beta\omega$ in Eq. (9) is equal to 1 in the most interesting frequency range $\beta\omega\ll 1$, which includes the central part of the peak of the low-frequency conductivity. The frequency dependence of the effective scattering rate and the conductivity in this range is determined by $S(q,\omega)$. On the other hand, in the analysis of the conductivity tail we will be interested primarily in the exponent, whereas

$[1-\exp(-\beta\omega)]/\beta\omega$ leads to a smooth frequency dependence of the prefactor ($\propto\omega^{-1}$ for $\beta\omega\gg1$). Therefore, we omit this factor in what follows.

B. The single-site approximation

Expression (9) is significantly simplified in the important and most common situation where the correlation length of the random potential r_c is small compared to the interelectron distance $n^{-1/2}$. Here, at most one electron is scattered by a given fluctuation of the potential, for example, by an impurity in the case of electrons in semiconductors or a short-wavelength ripplon in the case of electrons on helium. Since the 2DES is strongly correlated, all other electrons are far away.

The condition $r_c\ll n^{-1/2}$ allows us to single out the most important terms in the structure factor $\mathcal{S}(\mathbf{q},\omega)$. The major contribution to the sum over $\mathbf{q}$ in Eq. (9) comes from $q\sim\min(l^{-1},r_c^{-1})\gg n^{1/2}$. On the other hand, $\tilde{\mathcal{S}}(\mathbf{q},t)$ as given by Eq. (7) is a double sum of $\exp[i\mathbf{q}\cdot\mathbf{r}_m(t)]\exp[-i\mathbf{q}\cdot\mathbf{r}_{m'}(0)]$ over the electron numbers m,m'. The terms with $m\neq m'$ are rapidly oscillating for $q\gg n^{-1/2}$. Therefore, when calculating τ^{-1}, one should keep only diagonal terms with $m=m'$. We call this the single-site approximation,

$$\tilde{\mathcal{S}}(\mathbf{q},t)\approx\tilde{\mathcal{S}}_{ss}(\mathbf{q},t), \quad q\gg n^{1/2},$$

$$\tilde{\mathcal{S}}_{ss}(\mathbf{q},t)=\langle e^{i\mathbf{q}\cdot\mathbf{r}(t)}e^{-i\mathbf{q}\cdot\mathbf{r}(0)}\rangle_0, \quad (10)$$

where $\mathbf{r}\equiv\mathbf{r}_m$ stands for the coordinate of the mth electron. The result is independent of m, and therefore we disregarded the electron number in Eq. (10). Similarly, $\mathcal{S}(\mathbf{q},\omega)\approx\mathcal{S}_{ss}(\mathbf{q},\omega)$, where $\mathcal{S}_{ss}(\mathbf{q},\omega)$ is the Fourier transform of $\tilde{\mathcal{S}}_{ss}(\mathbf{q},t)$.

The transition from the Kubo formula (6) to Eqs. (8)–(10) corresponds to the approximation of independent scattering events for each individual electron. It is similar to the standard ladder approximation of the single-electron theory and is applicable, provided that the duration of a collision t_{col} is small compared to the reciprocal rate of electron scattering by the disorder potential. In turn, t_{col} is the typical time range that contributes to $\mathcal{S}_{ss}(\mathbf{q},\omega)$.

III. FREQUENCY DISPERSION OF THE CONDUCTIVITY: A SHORT-RANGE POTENTIAL

We will first consider the case of a short-range potential with correlation length

$$r_c\ll\delta_f\equiv(k_BT/m\omega_p^2)^{1/2}. \quad (11)$$

Here, δ_f is the typical thermal displacement of an electron from its quasiequilibrium position in the electron liquid. As explained in the Appendix, electron motion, on distances smaller than δ_f and for times much smaller than Ω^{-1}, is a transverse drift in a nearly uniform fluctuational electric field $\mathbf{E}_f$ (Ref. 20) [the electron vibration frequency Ω is given by Eq. (4)].

We will calculate the structure factor (10) using a formulation that differs from the one used in Ref. 15. It is advan-

tageous in the sense that it can be generalized to the case of multiple scattering by a disorder potential, as shown in Sec. IV.

Thermal averaging of a single-electron operator over the states of the many-electron system in Eq. (10) can be done in two steps. First, we average over the states of a given (mth) electron for a given many-electron configuration. Configuration averaging is done next. It is reduced to integration over the relative positions of the guiding centers $\mathbf{R}_{m'}$ of all other electrons ($m'\neq m$) with respect to $\mathbf{R}_m$. The integration has to be performed with the Boltzmann weighting factor exp $(-H_{ee}/k_BT)$ [see Eq. (A11)]. This is because the electron kinetic energies are eliminated by the Landau quantization, and the only relevant energy of the system is the potential energy of the electron-electron interaction.

The first averaging means taking a trace of a corresponding single-electron operator on the single-electron wave functions of an (mth) electron $\psi_k(\mathbf{r})$ ($\mathbf{r}\equiv\mathbf{r}_m$). The functions ψ_k belong to the lowest Landau level (LLL) and should be found assuming that the electron is in a uniform electric field $\mathbf{E}_f$ created by other electrons. No extra weighting factor (in particular, no Boltzmann factor) has to be incorporated when calculating the trace. The energy is determined only by the many-electron configuration, and thermal averaging is done over such configurations.

The wave functions $\psi_k(\mathbf{r})$ depend on the many-electron configurations only in terms of the fluctuational field $\mathbf{E}_f$. Therefore, the configuration averaging is reduced to averaging over the distribution of the field $\mathbf{E}_f$ (A3), which we denote by $\langle\cdots\rangle_{\mathbf{E}_f}$. Overall, the average value of a single-electron operator $O(\mathbf{r})$ can be written as

$$\langle O(\mathbf{r})\rangle=\frac{2\pi l^2}{S}\left\langle\sum_k\langle\psi_k(\mathbf{r})|O(\mathbf{r})|\psi_k(\mathbf{r})\rangle\right\rangle_{\mathbf{E}_f}, \quad (12)$$

where the prefactor is just the reciprocal number of states of the lowest Landau level.

In order to find the structure factor $\tilde{\mathcal{S}}_{ss}(\mathbf{q},t)$ [Eq. (10)] to the zeroth order in the random potential, we will use the explicit form of the LLL wave functions $\psi_k^{(0)}(\mathbf{r})$ of an electron in the field $\mathbf{E}_f$:

$$\psi_k^{(0)}(\mathbf{r})=\frac{1}{(L_yl)^{1/2}\pi^{1/4}}\exp\left(iky-\frac{1}{2l^2}(x-kl^2)^2\right). \quad (13)$$

Here, we chose the x axis in the direction of $\mathbf{E}_f$, i.e., $\mathbf{E}_f=E_f\hat{\mathbf{x}}$; L_y is the size of the system in the y direction, and the coordinate x is counted off from $-eE_f/m\omega_c^2$. The magnetic field is chosen along the negative z direction, $\mathbf{B}=-B\hat{\mathbf{z}}$.

The corresponding electron energy $\varepsilon_k^{(0)}$ (counted off from $\hbar\omega_c/2-e^2E_f^2/2m\omega_c^2$) is

$$\varepsilon_k^{(0)}=eE_fkl^2. \quad (14)$$

The structure factor (10) is determined by the trace of a product of the single-electron operators $\exp(\pm i\mathbf{q}\cdot\mathbf{r}(t))$ taken at different times in the Heisenberg representation. From Eqs. (13) and (14), we have

$$\langle\psi_k^{(0)}|e^{i\mathbf{q}\cdot\mathbf{r}(t)}e^{-i\mathbf{q}\cdot\mathbf{r}(0)}|\psi_k^{(0)}\rangle\approx e^{-q^2l^2/2}e^{it\mathbf{q}\cdot\mathbf{v}_D}, \qquad (15)$$

where $\mathbf{v}_D\equiv c\mathbf{E}_{\mathrm{f}}\times\mathbf{B}/B^2$ is the semiclassical drift velocity; for chosen axes, the, vector $\mathbf{v}_D$ points in the y direction. In Eq. (15), we disregarded fast-oscillating terms $\propto\exp(\pm in\omega_c t)$, with $n\geqslant 1$. Such terms make an extremely small contribution to the conductivity for $\omega\ll\omega_c$.

Following procedure (12), in order to find $\tilde{S}_{\mathrm{ss}}(\mathbf{q},t)$ we have to average the right-hand side of Eq. (15) over the fluctuational field $\mathbf{E}_{\mathrm{f}}$. For the Gaussian[10] field distribution (A3), this gives

$$\tilde{S}_{\mathrm{ss}}(\mathbf{q},t)=\exp\left[-\frac{1}{2}q^2l^2\left(1+\frac{t^2}{\tilde{t}_e^2}\right)\right]. \qquad (16)$$

Equation (16) shows that the structure factor decays very fast for wave numbers $q\gg 1/l$. For $ql\sim 1$, it also rapidly decays with time for $t\gg\tilde{t}_e$.

The characteristic time $\tilde{t}_e$ is simply related to the rms drift velocity and the rms fluctuational field $\langle E_{\mathrm{f}}^2\rangle$,

$$\tilde{t}_e=\frac{\sqrt{2}l}{\langle v_D^2\rangle^{1/2}}=\frac{\sqrt{2}\hbar}{el\langle E_{\mathrm{f}}^2\rangle^{1/2}} \qquad (17)$$

[the choice of the coefficients is convenient for Eq. (21) below]. A closely related time

$$t_e=l(B/c)\langle E_{\mathrm{f}}^{-1}\rangle\sim(\Omega k_B T/\hbar)^{-1/2} \qquad (18)$$

was introduced previously[15] as the average time of flight of an electron wave packet over a distance l in the crossed fields $\mathbf{E}_{\mathrm{f}}$ and $\mathbf{B}$. In the case of a short-range disorder potential ($r_c\ll l$), t_e is the duration of an electron collision with the fluctuation of the potential (a point defect). For a Gaussian distribution of the fluctuational field assumed here, we have $\tilde{t}_e=(2/\pi)^{1/2}t_e$.

Equations (9) and (16) give the conductivity in a simple form. The typical values of $\mathbf{q}$ transferred in an electron collision are $q_c=(r_c^2+l^2)^{-1/2}$. The duration of a collision is the time over which correlator (16) decays, t_e/q_cl. For a short-range potential (11), we have $t_e/q_cl\ll\Omega^{-1}$. This justifies the assumption that the fluctuational field remains constant during a collision, which is equivalent to the assumption that $t\ll\Omega^{-1}$.

The condition for the disorder potential to be weak, so that collisions occur successively in time, is

$$t_e[(r_c/l)^2+1]^{1/2}\ll\tau(0), \qquad (19)$$

where $\tau^{-1}(\omega)$ is given by Eq. (9) and is quadratic in the potential strength.

The typical frequency Ω [Eq. (4)] of electron vibrations about its quasiequilibrium position is also the rate of inter-electron energy exchange. The time interval between successive collisions of a vibrating electron with the same short-

range scatterer $\sim(q_c\delta_{\mathrm{f}})^2\Omega^{-1}$ is much larger than Ω^{-1}. Therefore, an electron loses coherence between successive collisions. This shows that interference effects leading to a weak localization in the single-electron approximation are not important for weak scattering.

A. The conductivity for a δ-correlated random potential

The expression for the conductivity can be obtained in an explicit form in the important case of a δ-correlated random potential $\overline{V(\mathbf{r})V(\mathbf{r}')}=v^2\delta(\mathbf{r}-\mathbf{r}')$ or

$$\overline{|V_{\mathbf{q}}|^2}=\pi\hbar^2\gamma^2l^2/2S, \quad \hbar\gamma=(2/\pi)^{1/2}v/l. \qquad (20)$$

The parameter $\gamma\propto 1/l$ introduced here is a convenient characteristic of the random potential in the problem of electrons in a quantizing magnetic field. It gives the width of the peak of the density of states $\rho(E)$ in the single-electron approximation;[21] in particular, on the tail $\rho(E)\propto\exp(-4E^2/\hbar^2\gamma^2)$, see Ref. 22. From Eq. (9), the scattering rate for the potential (20) is $\tau^{-1}(0)\sim\gamma^2t_e$, and the condition for the random potential to be weak takes a simple form

$$\gamma\ll t_e^{-1}.$$

Collecting Eqs. (8), (9), (16), and (20) we obtain a simple explicit expression for the frequency-dependent magnetoconductivity

$$\sigma_{xx}(\omega)\approx\frac{\pi}{16}\frac{ne^2\beta\gamma^2\tilde{t}_e}{m\omega_c}\sigma_1(\omega),$$

$$\sigma_1(\omega)=(1+\omega\tilde{t}_e)e^{-\omega\tilde{t}_e}. \qquad (21)$$

In the quasistatic limit of small ωt_e, Eq. (21) coincides with our previous result.[15] The conductivity $\sigma_{xx}(0)$ has a form of a single-electron conductivity in a magnetic field, with a scattering rate $\tau^{-1}\sim\gamma^2t_e$ quadratic in the disorder potential. However, in contrast to τ_{Dr}^{-1}, Eq. (2), the value of τ^{-1} is fully determined by the EEI. Through the factor t_e it depends on the fluctuational electric field that drives an electron during a collision with a scatterer. It scales with the density of the electron liquid as $n^{-3/4}$, so that the overall conductivity $\sigma_{xx}(0)\propto n^{1/4}$.

The frequency dependence of the conductivity is determined by the dimensionless function $\sigma_1(\omega)$, which is shown in Fig. 1. It peaks at zero frequency and monotonically decays with increasing ω. In contrast to the Drude conductivity in the absence of a magnetic field, which has a Lorentzian peak $\sigma_{xx}\propto 1/(1+\omega^2\tau^2)$, the peak of σ_1 is strongly non-Lorentzian. The characteristic width t_e^{-1} of the peak of σ_1 is *independent* of the disorder potential. Its dependence on the electron density, temperature, and the magnetic field is of the form $t_e^{-1}\propto n^{3/4}T^{1/2}B^{-1/2}$.

The tail of the peak is exponential in ω. Interestingly, it has the exact form of the Urbach rule,[23] i.e., $|\ln\sigma_1|\propto\omega$. [However, for very large ωt_e, where multiple scattering becomes important, this form is modified, see Sec. IV.] The shape of the tail can be understood by noticing that the conductivity is formed by processes in which the *energy* $\hbar\omega$ of
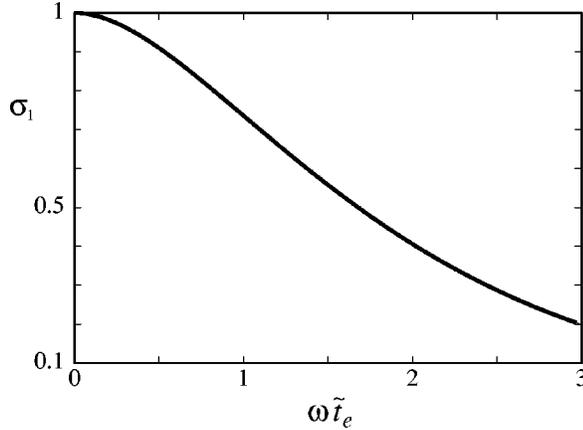
FIG. 1. The frequency dependence of the many-electron conductivity for a short-range disorder as given by Eq. (21).
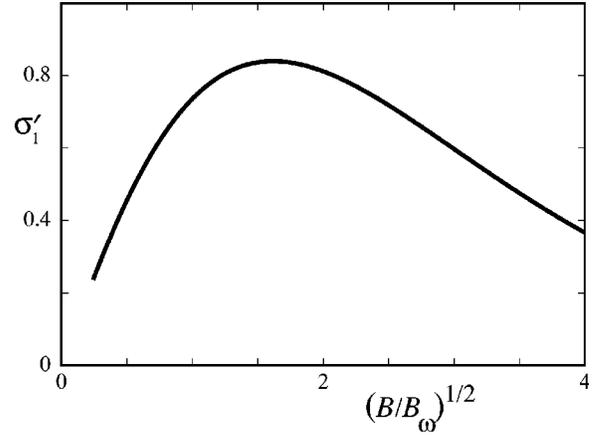

FIG. 2. The dependence of the reduced microwave many-electron conductivity $\sigma_1'(\omega) = \omega \tilde{t}_e \sigma_1(\omega)$ on the magnetic field for a weak δ-correlated random potential and for $k_B T \gg \hbar \omega$. Both the characteristic scaling magnetic field $B_\omega = B/(\omega \tilde{t}_e)^2$ and the ratio $\sigma_{xx}(\omega)/\sigma_1'(\omega)$ are independent of B, see Eqs. (17) and (21).

absorbed photons goes to the many-electron system. In an individual absorption process, the involved electron moves by the distance $\delta R = \hbar \omega / e |\mathbf{E}_f|$ along the fluctuational electric field $\mathbf{E}_f \| \hat{x}$. The squared matrix element of a dipolar electron transition accompanied by a displacement $\delta \mathbf{R} \equiv \delta R \, \hat{\mathbf{x}}$ is determined by the (squared) overlap integral of the wave functions (13):

$$|\langle \psi_k^{(0)}(\mathbf{r}) | \psi_k^{(0)}(\mathbf{r} + \delta \mathbf{R}) \rangle|^2 = \exp[-(\delta R)^2 / 2l^2]. \quad (22)$$

On the other hand, probability (A3) to have a fluctuational field $E_f = \hbar \omega / (e \, \delta R)$ is

$$p \propto \exp\left(- \frac{(\hbar \omega)^2}{e^2 (\delta R)^2 \langle E_f^2 \rangle} \right).$$

By optimizing the product of the two exponentials with respect to δR, we obtain that the conductivity is $\propto \exp(-\omega \tilde{t}_e)$, with expression (17) for $\tilde{t}_e$ taken into account. This is in agreement with Eq. (21).

It is important to check the assumption that the field $\mathbf{E}_f$ is uniform over relevant distances. In a strongly correlated system, $|\nabla \mathbf{E}_f| \sim e \, n^{3/2}$. Therefore for optimal δR and E_f, the relative change of the field on the distance δR is

$$\frac{|\nabla \mathbf{E}_f| \delta R}{E_f} \sim \frac{e \, n^{3/2} \delta R}{E_f} = \frac{e^2 n^{3/2} (\delta R)^2}{\hbar \omega} \sim \Omega t_e \ll 1.$$

It is interesting that this condition does not impose limitations on ω.

Another interesting feature of the many-electron microwave conductivity $\sigma_{xx}(\omega)$ is its nonmonotonic dependence on the magnetic field. Since $\gamma \propto 1/l \propto B^{1/2}$ [see Eq. (20)] and $t_e \propto B^{1/2}$ [Eq. (18)], the static conductivity $\sigma_{xx}(0) \propto B^{1/2}$ is *increasing* with B for quantizing fields. This happens because as B increases, the electron wave function becomes more localized, thus increasing the effective strength of coupling to short-range scatterers. At the same time, the electron drift velocity in the fluctuational field decreases, and as a result the characteristic collision duration t_e increases with B, lead-

ing to the overall scattering rate $\tau^{-1} \sim \gamma^2 t_e \propto B^{3/2}$.[15] The increase of $\sigma_{xx}(0)$ with increasing B has been confirmed experimentally.[16]

For nonzero frequencies, $\sigma_{xx}(\omega)$ displays a peak as a function of B, see Fig. 2. For comparatively small (but still quantizing) fields we have $\omega t_e \ll 1$, and then $\sigma_{xx}(\omega) \propto t_e \propto B^{1/2}$, as in the static limit. On the other hand, for B such that $\omega t_e \gg 1$, the conductivity falls down exponentially with increasing ωt_e. The position $B_{\max}$ of the peak of the conductivity is given by the Golden ratio

$$(\omega \tilde{t}_e)_{\max} = \frac{1 + \sqrt{5}}{2}, \quad B_{\max} \propto \omega^{-2}. \quad (23)$$

We note that the microwave magnetoconductivity displays a peak as a function of B in the single-electron approximation as well.[14] However, the shape of the peak is totally different. In particular, the high-B decay of the single-electron $\sigma_{xx}(\omega)$ is related to the localization of electron states in the random potential and is described by a power law. Many-electron effects lead to delocalization, and the decay of the conductivity with B becomes exponential, cf. Fig. 2. Of course, for very strong B the approximation of weak random potential $\gamma t_e \ll 1$ breaks down, and then the decay of $\sigma_{xx}(\omega)$ with B slows down.

We note also that in the single-electron theory, $\sigma_{xx}(0) = 0$ due to electron localization.[13,14] Therefore, $\sigma_{xx}(\omega)$ as a function of frequency has a peak at nonzero frequency which depends on B. This is in contrast with the monotonic decay of $\sigma_{xx}(\omega)$ in the many-electron theory shown in Fig. 1.

IV. CONDUCTIVITY TAIL: THE EFFECT OF MULTIPLE SCATTERING

It follows from the results of Sec. III [see Eq. (13)] that electron wave functions in crossed electric and magnetic fields display a Gaussian decay along the electric field. One may expect that multiple scattering of an electron in a short-

range random potential will slow down this decay, as it does for localized electrons in the absence of an electric field.[18] In turn, a slower spatial decay may lead to a slower decay of the many-electron conductivity $\sigma_{xx}(\omega)$ with frequency on the tail, where $\omega t_e \gg 1$. This is because it becomes more probable for an electron to shift by a larger distance along the fluctuational electric field $\mathbf{E}_f$ and, therefore, to absorb a photon with higher energy. The effect is similar to the impurity-mediated electron tunneling between the Landau levels tilted by an external electric field.[24,25]

The approximation of an electron moving in a static uniform field $\mathbf{E}_f$ is well justified in the frequency range $\omega t_e \gg 1$. Indeed, the many-electron field $\mathbf{E}_f$ changes over time $\sim \Omega^{-1}$, see the Appendix. It remains constant over the duration ω^{-1} of absorption of a photon because $\omega^{-1} \ll t_e \ll \Omega^{-1}$. The argument in favor of the field uniformity is based on the fact that the absorption tail is formed by large fields $\mathbf{E}_f$. They are experienced by electrons that are far away from their quasiequilibrium positions. The larger is the field, the larger the distance to the quasiequilibrium position should be. On the other hand, this distance is also the scale on which the field is spatially nonuniform. We will see that it will largely exceed the electron displacement $\hbar\omega/eE_f$ during absorption. Both lengths will be assumed much smaller than the interelectron distance $n^{-1/2}$.

A large electron displacement requires a large momentum transfer to the random potential, $q \gg n^{-1/2}$. Therefore, it is a good approximation to evaluate the correlator in the expression for conductivity (6) using the single-site approximation. This means that the product $\rho_{\mathbf{q}}(t)\rho_{\mathbf{q}'}(0)$ in Eq. (6) should be replaced by $\sum_m \exp[i\mathbf{q}\cdot\mathbf{r}_m(t)]\exp[i\mathbf{q}'\cdot\mathbf{r}_m(0)]$. Then

$$\sigma_{xx}(\omega) = -\frac{ne^2 l^4}{4 k_B T \hbar^2} \int_{-\infty}^{\infty} dt \, e^{i\omega t} \sum_{\mathbf{q},\mathbf{q}'} (\mathbf{q}\cdot\mathbf{q}')$$
$$\times \langle V_{\mathbf{q}} V_{\mathbf{q}'} e^{i\mathbf{q}\cdot\mathbf{r}(t)} e^{i\mathbf{q}'\cdot\mathbf{r}(0)} \rangle, \quad (24)$$

where $\mathbf{r} \equiv \mathbf{r}_m$ [the result is independent of the electron number m]. For $\hbar\omega \gtrsim k_B T$, we should replace $(k_B T)^{-1}$ with $[1 - \exp(-\beta\omega)]/\hbar\omega$; however, as noted above, it will only affect the prefactor in the conductivity.

The averaging in Eq. (24) can be done following prescription (12), i.e., one first calculates a trace over the single-electron wave functions ψ_k in a fluctuational field and then averages over the field. In contrast to the calculation in Sec. III, to allow for multiple scattering one should use wave functions found with the disorder potential $V(\mathbf{r})$ taken into account. In our approximation, averaging over realizations of $V(\mathbf{r})$ and $\mathbf{E}_f$ is done independently. It turns out to be more convenient to average over $V(\mathbf{r})$ first.

In what follows the random potential is assumed to be Gaussian and δ correlated, with correlator (20). We will use the Green-function technique. In contrast to what was done in the analysis of the tail of the wave function,[18] this technique has to be formulated in the frequency domain. We will show that this leads to a somewhat unusual set of diagrams.

A. The projected Green function

In order to find the low-frequency conductivity, it is convenient to use the Green function $G_\varepsilon(\mathbf{r},\mathbf{r}')$ "projected" on the lowest Landau level. It is constructed from the LLL wave functions $\psi_k(\mathbf{r})$ of an electron in the random potential $V(\mathbf{r})$ and in the electric field $\mathbf{E}_f$,

$$G_\varepsilon(\mathbf{r},\mathbf{r}') = \sum_k \psi_k(\mathbf{r})\psi_k^*(\mathbf{r}')(\varepsilon - i0 - \varepsilon_k)^{-1}, \quad (25)$$

where ε_k is the single-electron energy of the state k. The wave functions ψ_k are linear combinations of the LLL wave functions $\psi_k^{(0)}$ [Eq. (13)] in the absence of disorder. Following the averaging procedure (12), we obtain from Eq. (24),

$$\sigma_{xx}(\omega) = \frac{ne^2 l^4}{4 k_B T \hbar} \frac{l^2}{S} \mathrm{Re} \sum_{\nu=x,y} \int_{-\infty}^{\infty} d\varepsilon \int d\mathbf{r}\, d\mathbf{r}'$$
$$\times \langle V(\mathbf{r})V(\mathbf{r}')\, \partial_{r_\nu} \partial_{r'_\nu} G_\varepsilon(\mathbf{r},\mathbf{r}') G_{\varepsilon+\hbar\omega}^*(\mathbf{r},\mathbf{r}') \rangle_{\mathbf{E}_f}. \quad (26)$$

(Here, $\langle \dots \rangle_{\mathbf{E}_f}$ includes averaging over the random potential.)

We will consider the random potential $V(\mathbf{r})$ as a perturbation. The zeroth-order Green function $G_\varepsilon^{(0)}$ can be found using the explicit expressions (13) and (14) for the wave functions and the energy in the absence of disorder:

$$G_\varepsilon^{(0)}(\mathbf{r},\mathbf{r}') = \pi^{-1/2} l\, g(\mathbf{r},\mathbf{r}') \int dk$$
$$\times \frac{\exp(-[2l^2 k - (x+x') - i(y-y')]^2/4l^2)}{\varepsilon - eE_f l^2 k - i0}, \quad (27)$$

where the x axis is chosen along the field $\mathbf{E}_f$ as in Eq. (13).

The function

$$g(\mathbf{r},\mathbf{r}') = \frac{1}{2\pi l^2} e^{-(\mathbf{r}-\mathbf{r}')^2/4l^2}\, e^{i(x+x')(y-y')/2l^2} \quad (28)$$

in Eq. (27) has a simple meaning. It gives the (minus) right-hand side of the Schrödinger equation for the projected Green function $G_\varepsilon(\mathbf{r},\mathbf{r}')$, that is, it replaces the δ function $\delta(\mathbf{r}-\mathbf{r}')$ in the Schrödinger equation for a standard Green function. The function $g(\mathbf{r},\mathbf{r}')$ is localized in a narrow region $|\mathbf{r}-\mathbf{r}'| \lesssim 2l$ and leads to a Gaussian falloff of $G_\varepsilon^{(0)}$ for large distances.

The full Green function G_ε is determined by the Dyson equation. Its solution can be written symbolically as

$$G_\varepsilon = G_\varepsilon^{(0)} + G_\varepsilon^{(0)} \cdot V \cdot G_\varepsilon^{(0)} + G_\varepsilon^{(0)} \cdot V \cdot G_\varepsilon^{(0)} \cdot V \cdot G_\varepsilon^{(0)} + \cdots, \quad (29)$$

where the central dot implies integration over internal coordinates, such as $\int d\mathbf{r}_i G_\varepsilon^{(0)}(\mathbf{r}_{i-1},\mathbf{r}_i) V(\mathbf{r}_i) G_\varepsilon^{(0)}(\mathbf{r}_i,\mathbf{r}_{i+1})$. We emphasize that, even though the Green function G_ε is projected on the LLL, Eq. (29) contains the *full* rather than the projected disorder potential $V(\mathbf{r})$.

A straightforward calculation shows that, to the lowest order in V, the conductivity obtained from Eq. (26) coincides with the result of Sec. III; in this approximation, the full Green function G_ε in Eq. (26) has to be replaced with $G_\varepsilon^{(0)}$.
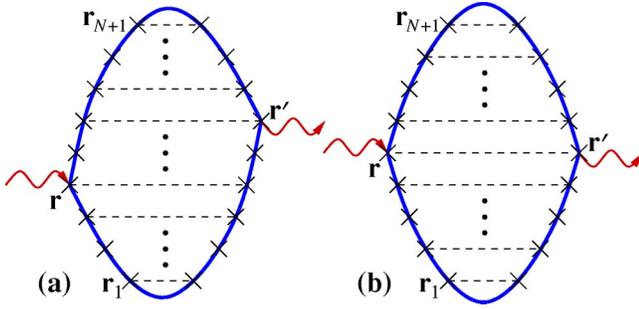
FIG. 3. Diagrams for conductivity (26) in the coordinate representation. Segments of the solid lines connecting the points $\mathbf{r} \equiv \mathbf{r}_s$ and $\mathbf{r}' \equiv \mathbf{r}_{s'}'$ in the upper and lower half planes are the Green functions $G_\varepsilon^{(0)}(\mathbf{r}_i, \mathbf{r}_{i+1})$ and $[G_{\varepsilon+\hbar\omega}^{(0)}(\mathbf{r}_i', \mathbf{r}_{i+1}')]^*$, respectively. Crosses (×) correspond to the Gaussian δ-correlated potential V at points $\mathbf{r}_i$ [subsequent integration over $\mathbf{r}_i$ is implied]. Dashed lines indicate averaging over V. Wavy lines mark the "external" vertices $V(\mathbf{r})$ and $V(\mathbf{r}')$ in Eq. (26) and imply differentiation of the product of the Green functions over $\mathbf{r}$, $\mathbf{r}'$ prior to averaging over V.

B. Diagrams for high-frequency conductivity

According to Eqs. (27) and (28), the Green function $G_\varepsilon^{(0)}(\mathbf{r}, \mathbf{r}')$ is mostly localized in a narrow region $|\mathbf{r} - \mathbf{r}'| \lesssim 2l$. As a function of energy, it peaks at the (scaled) midpoint in the $\mathbf{E}_f$ direction, where $\varepsilon = eE_f(x + x')/2$ for $y = y'$. Near the maximum,

$$G_\varepsilon^{(0)}(\mathbf{r}, \mathbf{r}') \approx \frac{g(\mathbf{r}, \mathbf{r}')}{\varepsilon - i0 - eE_f r^{(c)}},$$

$$r^{(c)} \equiv r^{(c)}(\mathbf{r}, \mathbf{r}') = [(x + x') + i(y - y')]/2. \quad (30)$$

With this in mind, we now consider expression (26) for the conductivity in terms of the product of the Green functions and assume that G_ε and G_ε^* are given by the perturbation series (29). In the product of the series, we need to find terms containing $G_\varepsilon^{(0)}(\mathbf{r}, \mathbf{r}')$ and $[G_{\varepsilon+\hbar\omega}^{(0)}(\tilde{\mathbf{r}}, \tilde{\mathbf{r}}')]^*$ with

$$eE_f[r^{(c)}(\tilde{\mathbf{r}}, \tilde{\mathbf{r}}') - r^{(c)}(\mathbf{r}, \mathbf{r}')] \approx \hbar\omega.$$

Such terms describe absorption of a photon accompanied by an electron displacement by $\delta R = \hbar\omega/eE_f$. The displacement results from scattering by the random potential.

Graphically, the leading-order contribution to conductivity can be represented by a sum of the "fat fish" diagrams illustrated in Fig. 3 in the coordinate representation. In this figure, the wavy lines mark the points $\mathbf{r}$ and $\mathbf{r}'$ where the derivatives of the product of the Green functions are taken in Eq. (26). The lines above and below these points represent series (29) for $G_\varepsilon(\mathbf{r}, \mathbf{r}')$ and $[G_{\varepsilon+\hbar\omega}(\mathbf{r}, \mathbf{r}')]^*$, respectively. The crosses (×) indicate the factors V in expansion (29) at points $\mathbf{r}_i$ where the electron is "scattered." Solid lines between the crosses denote the Green functions $G_\varepsilon^{(0)}(\mathbf{r}_i, \mathbf{r}_{i+1})$ and $[G_{\varepsilon+\hbar\omega}^{(0)}(\mathbf{r}_i', \mathbf{r}_{i+1}')]^*$ that describe electron propagation between collisions.

An Nth-order diagram has the total number of crosses equal to $2(N+1)$ (two crosses come from the external vertices in Fig. 3). We start with the Green functions that correspond to the top and bottom segments in Fig. 3. Each of them connects points with equal coordinates, $\mathbf{r}_{N+1}$ and $\mathbf{r}_1$, respectively. Their product is

$$G_\varepsilon^{(0)}(\mathbf{r}_1, \mathbf{r}_1)[G_{\varepsilon+\hbar\omega}^{(0)}(\mathbf{r}_{N+1}, \mathbf{r}_{N+1})]^*$$

$$\propto (\varepsilon - i0 - eE_f x_1)^{-1}(\varepsilon + \hbar\omega + i0 - eE_f x_{N+1})^{-1}. \quad (31)$$

Upon integration over ε in Eq. (26), expression (31) goes over into $2\pi^2\delta(\hbar\omega - eE_f(x_{N+1} - x_1))$. This is the equation of energy conservation in a photon-induced transition $\mathbf{r}_1 \rightarrow \mathbf{r}_{N+1}$. Such a transition is exactly the process that diagrams in Fig. 3 describe.

This picture provides a physical insight into the diagrams. It shows that the absorption does *not* occur in a transition $\mathbf{r} \rightarrow \mathbf{r}'$ between the external points of the diagram. Important for the transition is the admixture of the wave functions centered away from $\mathbf{r}$ and $\mathbf{r}'$ (in fact, maximally far away, see below).

The solid lines in Fig. 3 other than the top and bottom segments connect spatially separated points $\mathbf{r}_i$ and $\mathbf{r}_{i+1}$. The leading exponential terms in the dependence of the Green functions on the distance between the points is given by overlap functions $g(\mathbf{r}_i, \mathbf{r}_{i+1})$ [see Eq. (30)]. The product of the g functions entering the Nth-order diagrams can be written as

$$\tilde{g}_N(\{\mathbf{r}_j\}) = g(\mathbf{r}_1, \mathbf{r}_1)g(\mathbf{r}_{N+1}, \mathbf{r}_{N+1})\prod_{i=1}^{N}|g(\mathbf{r}_i, \mathbf{r}_{i+1})|^2$$

$$\propto \exp\left(-\sum_i (\mathbf{r}_i - \mathbf{r}_{i+1})^2/2l^2\right). \quad (32)$$

with $\{\mathbf{r}_j\} \equiv \mathbf{r}_1, \ldots, \mathbf{r}_{N+1}$. We have incorporated into Eq. (32) the terms from the "external" coordinates $\mathbf{r} \equiv \mathbf{r}_s$ and $\mathbf{r}' \equiv \mathbf{r}_{s'}'$.

For large $\hbar\omega/NeE_f l$, the integral over $\mathbf{r}_2, \ldots, \mathbf{r}_{N+1}$ can be evaluated by the steepest descent, with the constraint $\hbar\omega = eE_f(x_{N+1} - x_1)$ [the integral over $\mathbf{r}_1$ cancels the factor S^{-1} in Eq. (26)]. As in the case of underbarrier tunneling in a magnetic field,[18] the extreme points are equidistant:

$$x_i^{(e)} = x_1 + (i - 1)\hbar\omega/NeE_f, \quad y_i^{(e)} = y_1^{(e)} \quad (33)$$

for $i = 2, \ldots, N+1$. Then, at the extremum,

$$\ln \tilde{g}_N(\{\mathbf{r}_j^{(e)}\}) \approx -(\hbar\omega/eE_f l)^2/2N. \quad (34)$$

This expression has a simple physical meaning. The factor N in the denominator shows the scattering-induced increase of the overlap integral between the electron wave functions centered at points $\mathbf{r}_1$ and $\mathbf{r}_{N+1}$, which are separated by $\hbar\omega/eE_f$.

Except for the top and bottom Green functions (31), all other Green's functions in the diagrams in Fig. 3 are nonresonant. Their saddle-point values can be evaluated using the approximate expressions (30). The diagrams in Fig. 3(a) have $\mathbf{r}_s \equiv \mathbf{r}$ that differs from $\mathbf{r}_{s'} \equiv \mathbf{r}'$. These diagrams describe the interference of different tunneling paths and can be negative or positive. The total of all diagrams in Fig. 3 is, of

course, positive. The interference of paths affects only the prefactor in the conductivity. The leading exponential dependence on the distance $\hbar\omega/eE_f$ and on the diagram order N is not affected. It is the same for all diagrams in Fig. 3. Therefore, here we will give results only for the "diagonal" terms, which are described by the diagrams in Fig. 3(b).

The Nth -order diagrams in Fig. 3(b) contain a multiplier $[\pi\hbar^2\gamma^2l^2/2]^{N+1}$ from the intensity of the random potential (20). Together with the factors from the energy denominators [see Eq. (30)] and the factors from the integration over $d\mathbf{r}_i$ around the extreme points (33), these coefficients give an N-dependent factor

$$C_s=[N\gamma/\omega]^{2N}[(2s-3)!!(2N-2s+1)!!]^{-2},   \quad (35)$$

which also depends on the position s ($\mathbf{r}=\mathbf{r}'\equiv\mathbf{r}_s$) of the wavy lines in Fig. 3(b) (we assume that $1<s<N+1$). For large $N\gg1$, the factor C_s is maximal for $s=N/2$,

$$\ln C_{\max}\approx2N\ln(\gamma/\omega)+2N.   \quad (36)$$

The condition $s=N/2$ indicates that photon-induced transitions preferably occur between the states that are maximally (and equally) separated from the external points $\mathbf{r}$ and $\mathbf{r}'$. This is optimal in terms of maximizing the overlap integral of states with a given energy separation.

A more detailed calculation[26] shows that, in order to allow for the compensation from diagrams in Fig. 3(a), it is necessary to incorporate corrections to the leading-order steepest descent integrals. However, as we already mentioned, these corrections do not affect the leading term in $\ln\sigma_{xx}$. We also note that, for a given $\mathbf{E}_f$, the in-plane conductivity becomes anisotropic. This anisotropy leads to different prefactors for the conductivity in the directions parallel and perpendicular to $\mathbf{E}_f$.[26]

C. Frequency dependence of the logarithm of the conductivity

The logarithm of the conductivity $\sigma_{xx}(\omega)$ is given by the maximal value of the sum of expressions (34) and (36) with respect to the order of the diagram N. For $\omega=\omega_c$, the major factor in $\ln\sigma_{xx}(\omega)$ coincides with that in the logarithm of the inter-Landau-level tunneling rate in an external field in Ref. 24(b). To average over the fluctuational electric field, one has to add the logarithm of the field distribution and find the maximum of the resulting expression over $\mathbf{E}_f$. With the Gaussian field distribution (A3), we obtain

$$\ln\sigma_{xx}(\omega)\approx-(3/2^{1/3})(\omega\tilde{t}_e)^{2/3}[\ln(\omega/\gamma)-1]^{1/3},   \quad (37)$$

where $\tilde{t}_e$ is given by Eq. (17).

Equation (37) is the central result of this section. It shows that the logarithm of the conductivity depends on frequency as $\omega^{2/3}$ for large ω. This form of decay is a result of multiple scattering in the random potential, which helps an electron to move along the fluctuational field as it absorbs a photon. The crossover to Eq. (37) from the single-scattering approximation (21) (where $|\ln\sigma_{xx}|\propto\omega$) occurs when the optimal number of scattering events $N\sim(\omega t_e/\ln(\omega/\gamma))^{2/3}$ becomes large. The corresponding value of ω depends on both the many-electron fluctuational field and the intensity of the random potential.

Several comments need to be made about this result. First, the diagrams in Fig. 3 are unusual for a transport problem. They are neither the standard "ladder diagrams" nor the maximally crossing diagrams. Rather the diagrams in Fig. 3(b) are the maximally wrapped (embedded) diagrams for the self-energy. Here they appear, because absorption of a photon is accompanied by only one "real" scattering by the random potential. The role of multiple scattering is to alleviate the Gaussian decay of the electron wave function along the fluctuational field. Second, as the frequency increases, the probability of a realization of an optimal fluctuational field E_f may become non-Gaussian. In particular, in the region where $\ln p(E_f)$ is nearly linear in E_f,[10] we obtain $|\ln\sigma_{xx}|\propto\omega^{1/2}$, i.e., even a slower decay than Eq. (37).

V. MAGNETOCONDUCTIVITY IN A SMOOTH RANDOM POTENTIAL

In many physically interesting cases, the correlation length of the random potential r_c is large (or effectively large, see below) compared to the typical size of the electron wave packet. A well-known example is provided by electron systems in semiconductor heterostructures, where much of the disorder potential comes from the donors that are spatially separated from the 2DES. A sufficiently weak, smooth random potential does not lead to a glass transition in an electron liquid. The liquid should then display a nonzero static conductivity $\sigma_{xx}(0)$.

We are interested in the effect on transport of the dynamics of individual electrons in the electron liquid. We will consider scattering with a momentum transfer that largely exceeds the reciprocal interelectron distance $q\gg n^{-1/2}$. Such scattering is usually more important for magnetoconductivity. If, on the other hand, the random potential is smooth on the scale of the interelectron distance $r_c\gg n^{-1/2}$, the magnetoconductivity can be analyzed in the magnetohydrodynamic approximation by considering long-wavelength hydrodynamic modes of a viscous electron liquid in a magnetic field and a disorder potential.

A. Gaussian potential with correlation length $r_c\ll n^{-1/2}$

We start with the case of a weak Gaussian random potential with correlation length small compared to the interelectron distance. Here, to the second order in $V(\mathbf{r})$, the conductivity is given by Eqs. (8) and (9), with the structure factor $\mathcal{S}(\mathbf{q},\omega)$ evaluated in the single-site approximation (10).

The results become particularly interesting and instructive if the correlation length of the potential satisfies the condition

$$\delta_f\ll r_c\ll n^{-1/2},   \quad (38)$$

where δ_f is the thermal electron displacement from a quasi-equilibrium position in the liquid (11).

For a random potential that satisfies inequality (38), the structure factor $\tilde{\mathcal{S}}_{ss}(\mathbf{q},t)$ needs to be calculated for $q\ll1/\delta_f$. In other words, the electron displacement $|\mathbf{r}_m(t)-\mathbf{r}_m(0)|$ in Eq. (10) should exceed δ_f. Such displacements occur over times t that largely exceed the reciprocal frequency of vibrations about a quasiequilibrium position Ω^{-1}. They are due to
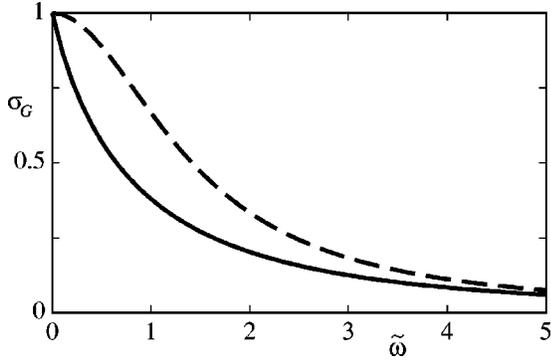
FIG. 4. Frequency dependence of the reduced microwave many-electron conductivity $\sigma_G(\omega)$ [Eq. (41)]. The scaled frequency is $\tilde{\omega} = \omega r_c^2/2D_{ee}$. The dashed line shows a Lorentzian curve with the same maximal value and the same asymptotic behavior for large ω.

self-diffusion in the electron liquid, with the diffusion coefficient D_{ee} (A14) introduced in the Appendix. In the diffusion approximation, we have

$$\tilde{\mathcal{S}}_{ss}(\mathbf{q},t) \approx \exp(-D_{ee}q^2|t|), \quad |t| \gg \Omega^{-1}. \quad (39)$$

The physical picture of scattering by a smooth random potential $V(\mathbf{r})$ is as follows. The guiding center of the electron cyclotron orbit drifts transverse to the sum of the many-electron fluctuational force $-e\mathbf{E}_f$ and $-\nabla V(\mathbf{r})$. The field $\mathbf{E}_f$ leads primarily to vibrations about a quasiequilibrium electron position. In turn, these vibrations result in partial averaging of the disorder potential. This is somewhat similar to motional narrowing in nuclear magnetic resonance. The averaging is incomplete because of self-diffusion of quasiequilibrium electron positions. Therefore, the momentum transferred to the disorder potential and, thus, the conductivity are determined by the diffusion rate.

Frequency dispersion of the conductivity depends on a specific model of the random potential. A model frequently used in the analysis of scattering of 2DES, including the quantum Hall effect, is a random potential with a Gaussian correlator,[12]

$$\overline{|V_\mathbf{q}|^2} = S^{-1} v_G^2 \exp(-q^2 r_c^2/2), \quad (40)$$

i.e., $\overline{V(\mathbf{r})V(\mathbf{r}')} = (v_G^2/2\pi r_c^2)\exp[-(\mathbf{r}-\mathbf{r}')^2/2r_c^2]$.

From Eqs. (8), (9), (39), and (40) we obtain for the magnetoconductivity,

$$\sigma_{xx}(\omega) = \frac{ne^2 v_G^2}{4\pi k_B T\, m^2 \omega_c^2 r_c^2 D_{ee}} \sigma_G(\omega),$$

$$\sigma_G(\omega) = 1 + \tilde{\omega}\left[\cos(\tilde{\omega})\left(\mathrm{Si}(\tilde{\omega}) - \frac{\pi}{2}\right) - \sin(\tilde{\omega})\mathrm{Ci}(\tilde{\omega})\right], \quad (41)$$

where $\tilde{\omega} = \omega r_c^2/2D_{ee}$, and $\mathrm{Si}(z)$ and $\mathrm{Ci}(z)$ are the sine and cosine integral functions, respectively.[27] Equation (41) is written for $\omega \geq 0$; the function $\sigma_{xx}(\omega)$ is even in ω.

The function $\sigma_G(\omega)$ is shown in Fig. 4. It decays monotonically with the increasing ω and has a Lorentzian-

type tail, $\sigma_G \approx 2/\tilde{\omega}^2$ for $\tilde{\omega} \gg 1$. An unusual feature of the conductivity is that σ_G is *linear* in $|\omega|$ for small $|\omega|$. It has the form $\sigma_G(0) - \text{const} \times |\omega|$. This nonanalytic behavior is a consequence of the slow decay of the structure factor $\tilde{\mathcal{S}}_{ss}(\mathbf{q},t)$ (39) with time for small wave numbers q. We note that Eq. (41) does not apply for very small $|\omega|$. Indeed, the single-site approximation (39) is valid only for $q \gg n^{1/2}$. This means that Eq. (41) can be used only for $|\omega| \gg D_{ee}n$ or $\tilde{\omega} \gg nr_c^2$.

The typical duration of a collision with the random potential is given by the time r_c^2/D_{ee} it takes for an electron to diffuse over the length r_c. The necessary condition for applicability of the above theory is that this time should be small compared to the relaxation time $\tau(0)$. It sets an upper bound on the strength of the disorder potential,

$$|v_G| \ll \hbar D_{ee}/l. \quad (42)$$

Inequality (42) can be understood by noticing that, as mentioned above, a smooth disorder potential adds to the electron drift velocity a term $i(c/eB)\Sigma_\mathbf{q}(\hat{\mathbf{z}} \times \mathbf{q}) V_\mathbf{q}\exp(i\mathbf{q}\cdot\mathbf{r})$. Equation (42) corresponds to the condition that the root-mean-square electron displacement due to this velocity over the collision duration r_c^2/D_{ee} should be small compared to the size of the electron wave packet l. Interestingly, the correlation length r_c drops out of Eq. (42).

The parameter range, where a 2D electron system forms a liquid, is not limited to temperatures where electron motion is semiclassical, $k_B T \gg \hbar\Omega$ (4). The results of this section are valid even for $k_B T < \hbar\Omega$ as long as the electron system displays self-diffusion. The parameter δ_f in inequality (38) is in this case determined by quantum zero-point fluctuations.

The formalism of this section can be applied also to the case of a smooth potential created by charged donors separated from the electron layer by a spacer of width $d \ll n^{-1/2}$. The major contribution to the conductivity comes from the scattering with momentum transfer $\sim \hbar/d$. However, the long-wavelength tail of the Coulomb potential leads to a logarithmic divergence of the relaxation rate $\tau^{-1}(0)$ calculated using Eqs. (9) and (39). The analysis of this divergence requires a hydrodynamic approach and will be carried out in a separate paper.

B. Electron traps

An important type of disorder, particularly for metal-oxide-semiconductor systems, are electron traps. One can think of them as deep short-range potential wells $V_{tr}(\mathbf{r})$ located at random positions $\boldsymbol{\rho}_\kappa$. The overall random potential then is

$$V(\mathbf{r}) = \sum_\kappa V_{tr}(\mathbf{r} - \boldsymbol{\rho}_\kappa). \quad (43)$$

The potentials V_{tr} are not weak, but the trap density N_{tr} is assumed small. In particular, we assume that the intertrap distance $N_{tr}^{-1/2}$ largely exceeds the correlation length of the electron liquid. Then, even though the traps will capture

some electrons, other electrons will be free to move and there still will be self-diffusion in the electron liquid.

To the lowest order in N_{tr}, the magnetoconductivity is given by Eq. (6). For $\hbar\omega\ll k_B T$, we write it in the form

$$\sigma_{xx}(\omega)=\frac{e^2 l^4}{4 k_B T \hbar^2 S}\sum_{n,n'}\ \sum_{\kappa,\kappa'}\ \int_{-\infty}^{\infty}dt\ e^{i\omega t}$$
$$\times\langle\boldsymbol{\nabla}_n V_{\mathrm{tr}}[\mathbf{r}_n(t)-\boldsymbol{\rho}_\kappa]\cdot\boldsymbol{\nabla}_{n'}V_{\mathrm{tr}}[\mathbf{r}_n'(0)-\boldsymbol{\rho}_{\kappa'}]\rangle.$$
(44)

Because electrons are strongly correlated, only one electron may experience the potential of a given trap at a time. We assume that this electron gets localized on the trap. It then creates a repulsive Coulomb potential for other electrons, and they stay away from the trap.

The picture of one localized electron per trap allows us to rewrite the sum of the correlation functions in Eq. (44) as

$$\sum_{n,n'}\ \sum_{\kappa,\kappa'}\langle\cdots\rangle\to\sum_\kappa\ \langle\boldsymbol{\nabla}_\kappa V_{\mathrm{tr}}[\mathbf{r}_\kappa(t)]\cdot\boldsymbol{\nabla}_\kappa V_{\mathrm{tr}}[\mathbf{r}_\kappa(0)]\rangle.$$
(45)

Here, $\mathbf{r}_\kappa$ is the coordinate of an electron on a κth trap counted off from the trap position $\boldsymbol{\rho}_\kappa$. We also disregarded terms with $\kappa'\neq\kappa$, because different traps are far from each other and electrons on different traps are not correlated.

We will assume that a localized electron occupies only the ground bound state $|g\rangle$ in the potential $V_{\mathrm{tr}}(\mathbf{r})$ and that the energy spacing between the ground state and the nearest excited state is $\hbar\omega_{g\to e}\gg k_B T$. Then electrons very rarely escape from the traps or are thermally excited to higher states. It should be noted that, in fact, the true binding potential is stronger than the "bare" potential V_{tr}, because surrounding electrons contribute to electron localization by providing a "caging" potential. The localization length of the state $|g\rangle$ in a quantizing magnetic field is of the order of the magnetic length $l\ll\delta_{\mathrm{f}}$.

For $\hbar\omega_{g\to e}\gg k_B T$, thermal averaging of a single-electron operator $\hat{O}\equiv O(\mathbf{r}_\kappa)$ in Eq. (45) is done in two steps. First, one has to find the diagonal matrix element $\langle g|\hat{O}|g\rangle$ on the wave functions of the ground state of the trapped electron. Then the matrix element has to be averaged over the states of the many-electron system. In addition, if we are interested in the conductivity at frequencies $\omega\ll\omega_{g\to e}$, we have

$$\langle g|\boldsymbol{\nabla}_\kappa V_{\mathrm{tr}}[\mathbf{r}_\kappa(t)]\cdot\boldsymbol{\nabla}_\kappa V_{\mathrm{tr}}[\mathbf{r}_\kappa(0)]|g\rangle$$
$$\to\langle g|\boldsymbol{\nabla}_\kappa V_{\mathrm{tr}}[\mathbf{r}_\kappa(t)]|g\rangle\langle g|\boldsymbol{\nabla}_\kappa V_{\mathrm{tr}}[\mathbf{r}_\kappa(0)]|g\rangle.$$

In order to calculate the matrix elements $\langle g|\boldsymbol{\nabla}_\kappa V_{\mathrm{tr}}(\mathbf{r}_\kappa)|g\rangle$, we note that, besides the potential of the defect, a trapped electron experiences a potential from other electrons. The fluctuating part of this potential varies on time $\sim\Omega^{-1}$. In the range of interest, $\beta\Omega\ll 1$ (4) and $\beta\omega_{g\to e}\gg 1$, we have $\Omega\ll\omega_{g\to e}$. Therefore, a localized electron follows the many-electron field adiabatically. The overall force on a κth localized electron is $-\boldsymbol{\nabla}V_{\mathrm{tr}}(\mathbf{r}_\kappa)-e\mathbf{E}_\kappa$, where $\mathbf{E}_\kappa$ is the many-electron fluctuational field on this electron (see the

Appendix). The diagonal matrix element of the force should be equal to zero. This gives for correlator (45),

$$\langle\boldsymbol{\nabla}_\kappa V_{\mathrm{tr}}[\mathbf{r}_\kappa(t)]\cdot\boldsymbol{\nabla}_\kappa V_{\mathrm{tr}}[\mathbf{r}_\kappa(0)]\rangle=e^2\langle\mathbf{E}_\kappa(t)\mathbf{E}_\kappa(0)\rangle.$$
(46)

For a trapped electron, the behavior of $\langle\mathbf{E}_\kappa(t)\mathbf{E}_\kappa(0)\rangle$ is determined by the motion of neighboring electrons. As in the absence of trapping, this motion comprises vibrations about quasiequilibrium positions superimposed on diffusion of these positions. Because the trapped electron itself does not move, the vibrations and the diffusion are somewhat different from those in the free-electron liquid. However, we do not expect this difference to be too large. Indeed, a neighbor of a trapped electron has at most one of its six (on average) nearest neighbors localized. Therefore, the correlator $\langle\mathbf{E}_\kappa(t)\mathbf{E}_\kappa(0)\rangle$ should still decay on times of the order of the reciprocal vibration frequency Ω^{-1}, in the central part.

It is seen from Eqs. (44) and (46) that $\sigma_{xx}(0)$ is determined by the integral of the field correlator over time, with no extra time-dependent weight. In the semiclassical approximation, this integral is simply related to the self-diffusion coefficient D_{ee} of the electron liquid (A12) and (A13). For a trapped electron, it should be the same, to the order of magnitude, and may only differ by a factor ~ 1 that depends on Γ. Therefore,

$$\sigma_{xx}(0)\sim N_{\mathrm{tr}}\ e^2 D_{ee}/k_B T.$$
(47)

In contrast to the cases discussed before, the conductivity $\sigma_{xx}(\omega)$ does not peak at $\omega=0$ for low frequencies. The field power spectrum, which is given by the Fourier transform of correlator (46), increases with ω. A simple calculation shows that, for a Wigner crystal, this increase is linear for $\omega\ll\Omega$. Therefore, for an electron liquid it should be linear in the range $\delta_{\mathrm{f}}^2/D_{ee}\ll\omega\ll\Omega$. The conductivity peaks at $\omega\sim\Omega$. The overall width of the peak of the low-frequency conductivity is $\sim\Omega$.

Equation (47) shows that, for short-range traps, magnetoconductivity is proportional to the defect density, rather than the electron density n. For $\omega=0$, it depends on n only in terms of the self-diffusion coefficient D_{ee}. The shape of the peak also depends on n. Therefore, measurements of the conductivity spectrum should provide an insight into both long- and short-time electron dynamics in the liquid, i.e., self-diffusion and vibrations about quasiequilibrium positions. We note the similarity between this problem and the problem of dissipative conductivity of a 2D superconducting film with vortices in the presence of pinning centers.

VI. CONCLUSIONS

In this paper, we have found the frequency dependence of the conductivity of a nondegenerate electron liquid in a quantizing magnetic field for $\omega\ll\omega_c$. We have shown that this dependence is extremely sensitive to both short- and long-time electron dynamics in the liquid and the characteristics of the random potential.

For a short-range potential, the conductivity is determined by a large-$\mathbf{q}$ electron scattering. It occurs as an electron drifts transverse to the magnetic field and the field $\mathbf{E}_{\mathrm{f}}$, which is

created by density fluctuations in the liquid. The results become particularly simple if the correlation length of the potential r_c is less than the magnetic length l. Here, the shape of the peak of $\sigma_{xx}(\omega)$ depends on one dimensionless parameter ωt_e and is given by an explicit expression (21). The time t_e is the time of flight over the length l in the field $\mathbf{E}_f$. It is smaller than the inverse rate of interelectron momentum exchange Ω^{-1} and depends on the electron density, temperature, and magnetic field as $t_e \propto n^{-3/4}T^{-1/2}B^{1/2}$. Therefore, by studying the shape of the magnetoconductivity peak for a short-range disorder one can investigate the short-time electron dynamics as a function of the parameters of the electron liquid.

The tail of the conductivity in the range $t_e^{-1} \ll \omega \ll \omega_c$ is exponential and obeys the Urbach rule. The photon energy $\hbar \omega$ is transferred to the many-electron system via a radiation-induced electron displacement along the field $\mathbf{E}_f$. The momentum needed for the displacement comes from scattering by a fluctuation of the disorder potential. As ωt_e increases, it becomes more probable for an electron to experience multiple scattering. This leads to the change of the asymptotic behavior from $|\ln \sigma_{xx}| \propto \omega$ to $|\ln \sigma_{xx}| \propto \omega^{2/3}$. Such behavior is described by unusual fat fish diagrams, which correspond to maximally embedded diagrams in the self-energy (see Fig. 3).

The conductivity has a different form for a long-range disorder potential. Of particular interest is the case where the correlation length r_c exceeds the root-mean-square electron displacement from a quasiequilibrium position in the liquid δ_f. Here, $\sigma_{xx}(\omega)$ is determined by electron diffusion in the liquid. It has a simple form given by Eq. (41). The shape of the spectral peak of $\sigma_{xx}(\omega)$ depends on one dimensionless parameter $\omega r_c^2/D_{ee}$. It displays a rounded cusp at $\omega = 0$ and decays as ω^{-2} for large $\omega r_c^2/D_{ee}$.

Yet, another behavior arises in the case where scatterers are short-range electron traps. If the density of the trapped electrons is small, the 2DES remains a liquid. The conductivity is expressed in terms of the power spectrum of the fluctuational field $\mathbf{E}_f$ that the liquid exerts on a trapped electron. The spectral peak of the conductivity is located at a frequency $\sim \Omega$. The low-frequency part of the peak is determined by electron diffusion, whereas the shape of the peak near its maximum depends on vibrations of electrons about their quasiequilibrium positions in the liquid.

ACKNOWLEDGMENTS

APPENDIX: DYNAMICS OF A NONDEGENERATE 2D ELECTRON LIQUID

A snapshot of a correlated 2D electron liquid is shown schematically in Fig. 1(a). In such a liquid, for most of the time, the electrons perform small-amplitude vibrations about their quasiequilibrium positions in the potential formed by other electrons and the neutralizing background. In the absence of a magnetic field, the characteristic frequency of
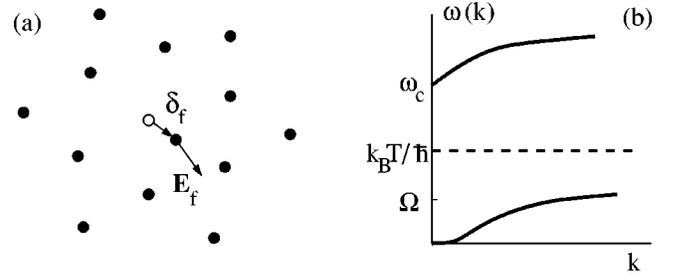

FIG. 5. (a) A snapshot of a correlated electron fluid (schematically). The open circle shows an equilibrium position of one of the electrons in the field of other electrons. Because the electron is displaced, it experiences a restoring force, which is determined by the fluctuational electric field $\mathbf{E}_f$. (b) Phonon spectrum of a 2D Wigner crystal in a quantizing magnetic field (schematically).

such vibrations is determined by the second derivative of the Coulomb potential at the mean interelectron distance $n^{-1/2}$ and is given by the short-wavelength plasma frequency $\omega_p = (2\pi e^2 n^{3/2}/m)^{1/2}$, which is the characteristic Debye frequency of a 2D Wigner crystal.

An important characteristic of electron dynamics is the typical fluctuational electron displacement from the quasi-equilibrium position δ_f in Fig. 5(a). If the electron motion is classical, i.e., for $\hbar\omega_p \ll k_B T$, it can be estimated in the harmonic approximation by setting the potential energy $e^2 n^{3/2} \delta_f^2$ equal to $k_B T$:

$$\langle \delta_f^2 \rangle = k_B T / e^2 n^{3/2}. \tag{A1}$$

The necessary condition that δ_f^2 be much less than the squared interelectron distance n^{-1} is equivalent to $\Gamma \gg 1$.

The restoring force on the vibrating electron is given by the electric field $\mathbf{E}_f$, see Fig. 5a. This field is due to electron-density fluctuations. In the classical regime, these are primarily short-wavelength fluctuations.[15] For large Γ, the field should be close to its value estimated in the harmonic approximation in electron displacements from quasiequilibrium positions,

$$\langle E_f^2 \rangle = F(\Gamma) n^{3/2} k_B T. \tag{A2}$$

The function $F(\Gamma)$ was obtained by Monte Carlo simulations.[10] In the whole range $10 < \Gamma < \Gamma_W = 130$ it remains essentially constant, varying from 10.5 to 9.1. The field distribution $p(\mathbf{E}_f)$ is Gaussian in the central part:

$$p(\mathbf{E}_f) = [\pi \langle E_f^2 \rangle]^{-1} \exp[-E_f^2/\langle E_f^2 \rangle], \tag{A3}$$

which is an indication that, in this range of Γ, the electron motion is mostly weakly anharmonic vibrations. On the far tail, the decay of $p(\mathbf{E}_f)$ is slowed down compared to Eq. (A3).[10] The fluctuational field is the only characteristic of the electron liquid, which is needed in order to describe the magnetoconductivity $\sigma_{xx}(\omega)$ in the case of a weak short-range disorder.

1. A nondegenerate electron liquid in a strong magnetic field

In a strong magnetic field, $\omega_c \gg \omega_p$, the electron motion is separated into cyclotron motion with frequencies $\sim \omega_c$ and comparatively slow vibrations of the guiding centers about their slowly diffusing quasiequilibrium positions. The coordinates of the guiding centers are

$$\mathbf{R}_n = (X_n, Y_n), \quad \mathbf{R}_n = \mathbf{r}_n + \hbar^{-1} l^2 \mathbf{p} \times \hat{\mathbf{z}}, \quad \text{(A4)}$$

where, $\hat{\mathbf{z}} = -\mathbf{B}/B$ is the unit vector normal to the electron layer, and $\mathbf{p}$ is the canonical momentum. From Eq. (A4), the components X_n, Y_n obey the commutation relation

$$[X_n, Y_n] = -il^2, \quad l^2 = \hbar/(m\omega_c). \quad \text{(A5)}$$

The magnetic length l gives the typical size of the electron wave packet.

The dynamics of the guiding centers is described by the Hamiltonian of the electron-electron interaction H_{ee} (3) projected on the lowest Landau level,

$$H_{ee} \approx \frac{e^2}{2} \sum_{n \neq m} |\mathbf{R}_n - \mathbf{R}_m|^{-1}. \quad \text{(A6)}$$

The Heisenberg equations of motion for $\mathbf{R}_n$ can be written in a closed form in the important case where the electric field on electrons is smooth on the scale l:

$$\dot{\mathbf{R}}_n = cB^{-2} \mathbf{E}_n \times \mathbf{B}. \quad \text{(A7)}$$

Here,

$$\mathbf{E}_n = e \frac{\partial}{\partial \mathbf{R}_n} \sum_{m(m \neq n)} |\mathbf{R}_n - \mathbf{R}_m|^{-1} \quad \text{(A8)}$$

is the field on the nth electron created by other electrons and calculated by ignoring noncommutativity (A5) of the guiding centers' components.

By linearizing $\mathbf{E}_n$ in displacements of the electrons from their quasiequilibrium positions, one can see that the motion of the guiding centers comprises mostly vibrations with a typical frequency

$$\Omega = \omega_p^2/\omega_c = 2\pi e^2 n^{3/2}/m\omega_c. \quad \text{(A9)}$$

This frequency also gives the typical rate of interelectron momentum exchange. In the case where electrons form a Wigner crystal, Ω is the zone-boundary frequency of the lower phonon branch, see Fig. 5(b).

Motion of the guiding centers $\mathbf{R}_n$ becomes semiclassical for

$$k_B T \gg \hbar \Omega. \quad \text{(A10)}$$

It is determined by thermal fluctuations. From Eq. (A10), a typical electron displacement from a quasiequilibrium position δ_f given by Eq. (A1) is $\delta_f \gg l$. Therefore, the fluctuational electric field $\mathbf{E}_f$, which varies on the distance δ_f, is uniform on the magnetic length l, as assumed in Eq. (A7).

The probability distribution of the guiding centers $\rho(\mathbf{R}_1, \ldots, \mathbf{R}_n, \ldots)$ is given by the Boltzmann equation

$$\rho(\mathbf{R}_1, \ldots, \mathbf{R}_n, \ldots) = \text{const} \times \exp(-H_{ee}/k_B T), \quad \text{(A11)}$$

with H_{ee} given by Eq. (A6). Therefore, the results for a classical electron liquid in the absence of a magnetic field can now be carried over to the case of quantizing magnetic field. In particular, the instantaneous distribution of the fluctuational field $\mathbf{E}_f$ is the same as in the classical 2DES for $B = 0$. Condition (A10) is much less restrictive than $\hbar\omega_p \ll k_B T$ because $\Omega \ll \omega_p$.

For $\Gamma < 130$, Eqs. (A7), (A8), and (A11) provide a semiclassical description of a nondegenerate electron liquid in a strong magnetic field. In the long-wavelength limit, this liquid can be alternatively described in the hydrodynamic approximation. The transport coefficients (e.g., viscosity) can be found from the correlation functions of the liquid (e.g., current-current correlator). In two dimensions, because of a large contribution from long-wavelength modes, the transport coefficients diverge. A self-consistent analysis in the case of a classical 2D liquid for small frequencies ω and wave numbers q was done by Andreev.[28] He showed that transport coefficients diverge as $\ln^{1/2}\omega$ in the limit of small ω. For a 2D electron liquid in a short-wavelength random potential, this divergence is terminated at the cutoff frequency given by the rate of electron scattering in this potential τ^{-1}. This rate determines the long-wavelength static conductivity and thus the decay rate of long-wavelength modes of the electron liquid. A corresponding self-consistent analysis in the presence of a magnetic field will be given elsewhere. A logarithmic correction to the viscosity of a 2D Fermi liquid due to electron-impurity scattering was found in Ref. 29.

An important feature of the liquid state, which ultimately gives rise to a nonzero static conductivity, is self-diffusion. The coefficient of self-diffusion D_{ee} can be related to the rms displacement of a particle over a long time $t \gg \Omega^{-1}$,

$$D_{ee} = \Delta R_n^2(t)/4t, \quad \Delta R_n^2(t) \equiv \langle [\mathbf{R}_n(t) - \mathbf{R}_n(0)]^2 \rangle. \quad \text{(A12)}$$

If we assume that the semiclassical approximation (A7) applies for long times $t \gg \Omega^{-1}$, then the electron displacement is related to the correlator of the fluctuational electric field by

$$\Delta R_n^2(t) = (c/B)^2 \int_0^t dt' \int_0^t dt'' \langle \mathbf{E}_n(t') \mathbf{E}_n(t'') \rangle. \quad \text{(A13)}$$

The natural scale of the electric field is given by the rms value (A2). Field correlations decay over the time $\sim \Omega^{-1}$. Then, the diffusion coefficient becomes

$$D_{ee} = \frac{k_B T}{m\omega_c} \widetilde{D}_{ee}(\Gamma, \Omega t). \quad \text{(A14)}$$

Here, we took into account that $c^2 \langle E_f^2 \rangle/B^2\Omega \sim k_B T/m\omega_c$.

We note that, in the absence of a magnetic field, the power spectrum of the field $\mathbf{E}_f$ goes to zero for $\omega \to 0$. In this case, the double integral over time in Eq. (A13) gives just the average increment of the momentum of an electron, which saturates for large t. The electron dynamics in a magnetic field is different, and we expect that here the integral (A13)

linearly increases with t. This conjecture is based on the argument that, because of self-diffusion in the electron liquid, $\Delta R_n^2(t)$ should linearly increase in time. This increase must be caused by the fluctuational field, since quantum corrections to an electron displacement are small.[15]

An analysis based on magnetohydrodynamics with a frequency-independent viscosity coefficient leads to an extra factor $\ln t$ in the time dependence of $\Delta R_n^2(t)$. A similar factor should arise in the function $\tilde{D}_{ee}$ for $t \ll \tau$. However, it should saturate and become a constant for $t > \tau$. For a correlated liquid, we expect that the factor $\tilde{D}_{ee}$ is not large, $\tilde{D}_{ee} \lesssim 1$.

In the absence of a magnetic field, straightforward scaling arguments give an expression of the type (A14) for the self-diffusion coefficient, with ω_c replaced by the characteristic vibration frequency ω_p. The numerical factor that stands for $\tilde{D}_{ee}$ in this expression is known from the data of simulations,[7–10] it is ~ 0.1 close to the melting transition and increases with temperature.

---

*Email address: dykman@pa.msu.edu

†Email address: leonid@landau.ucr.edu

[1] *Perspectives in Quantum Hall Effects*, edited by S. Das Sarma and A. Pinczuk (Wiley, New York, 1997).

[2] E. Abrahams, S.V. Kravchenko, and M.P. Sarachik, Rev. Mod. Phys. **73**, 251 (2002).

[3] B. Tanatar and D.M. Ceperley, Phys. Rev. B **39**, 5005 (1989).

[4] *Two-dimensional Electron Systems on Helium and Other Cryogenic Substrates*, edited by E.Y. Andrei (Kluwer, Boston, 1997).

[5] See S. Chakravarty, S. Kivelson, Ch. Nayak, and K. Voelker, Philos. Mag. B **79**, 859 (1999); B. Spivak, Phys. Rev. B **67**, 125205 (2002).

[6] For recent work, see H. Noh, M.P. Lilly, D.C. Tsui, J.A. Simmons, L.N. Pfeiffer, and K. W. West, cond-mat/0301301 (unpublished).

[7] J.P. Hansen, D. Levesque, and J.J. Weis, Phys. Rev. Lett. **43**, 979 (1979).

[8] R.K. Kalia, P. Vashishta, and S.W. de Leeuw, Phys. Rev. B **23**, 4794 (1981).

[9] K.J. Strandburg, Rev. Mod. Phys. **60**, 161 (1988).

[10] C. Fang-Yen, M.I. Dykman, and M.J. Lea, Phys. Rev. B **55**, 16 272 (1997).

[11] A. Pruisken, in *The Quantum Hall effect*, edited by R. Prange and S.M. Girvin (Springer, New York, 1990), p. 117.

[12] B. Huckestein, Rev. Mod. Phys. **67**, 357 (1995).

[13] Z.-Q. Wang, Matthew P.A. Fisher, S.M. Girvin, and J.T. Chalker, Phys. Rev. B **61**, 8326 (2000).

[14] F. Kuehnel, L.P. Pryadko, and M.I. Dykman, Phys. Rev. B **63**, 165326 (2001).

[15] M.I. Dykman and L.S. Khazan, Zh. Eksp. Teor. Fiz. **77**, 1488 (1979) [JETP **50**, 747 (1979)]; M.I. Dykman, M.J. Lea, P. Fozooni, and J. Frost, Phys. Rev. Lett. **70**, 3975 (1993); M.I. Dykman, C. Fang-Yen, and M.J. Lea, Phys. Rev. B **55**, 16 249 (1997).

[16] M.J. Lea, P. Fozooni, A. Kristensen, P.J. Richardson, K. Djerfi, M.I. Dykman, C. Fang-Yen, and A. Blackburn, Phys. Rev. B **55**, 16 280 (1997); M.J. Lea and M.I. Dykman, Physica B **251**, 628 (1998), and references therein.

[17] E. Teske, Yu.P. Monarkha, M. Seck, and P. Wyder, Phys. Rev. Lett. **82**, 2772 (1999).

[18] B.I. Shklovskii, Pis'ma Zh. Eksp. Teor. Fiz. **36**, 43 (1982) [JETP Lett. **36**, 51 (1982)]; B.I. Shklovskii and A.L. Efros, Zh. Eksp. Teor. Fiz. **84**, 811 (1983) [JETP **57**, 470 (1983)]. Qin Li and D.J. Thouless, Phys. Rev. B **40**, 9738 (1989); T. Martin and S. Feng, *ibid.* **44**, 9084 (1991); J. Hajdu, M.E. Raikh, and T.V. Shahbazyan, *ibid.* **50**, 17 625 (1994).

[19] The problem of elementary excitations in a strongly correlated 3D liquid with a screened Coulomb interaction has been addressed recently by several groups in the context of dust particles in plasma, see H. Ohta and S. Hamaguchi, Phys. Rev. Lett. **84**, 6026 (2000); G. Kalman, M. Rosenberg, and H.E. DeWitt, *ibid.* **84**, 6030 (2000), and references therein.

[20] Fluctuational field on an electron in a correlated electron liquid is totally different from the fluctuational field in a weakly nonideal electron plasma discussed, for example, in the context of the effect of the electron-electron interaction on weak localization, see B.L. Altshuler and A.G. Aronov, in *Electron-Electron Interaction in Disordered Systems*, edited by A.L. Efros and M. Pollak (North-Holland, Amsterdam, 1985).

[21] F. Wegner, Zh. Eksp. Teor. Fiz. **81**, 1048 (1981) [Z. Phys. B: Condens. Matter **51**, 279 (1983)].

[22] L.B. Ioffe and A.I. Larkin, Zh. Eksp. Teor. Fiz. **81**, 1048 (1981) [JETP **54**, 556 (1981)].

[23] F. Urbach, Phys. Rev. **92**, 1324 (1953).

[24] V.L. Pokrovsky, L.P. Pryadko, and A.L. Talapov, Zh. Eksp. Teor. Fiz. **95**, 668 (1989) [JETP **68**, 376 (1989)].

[25] D. Polyakov and M. Raikh, Solid State Commun. **74**, 1209 (1990).

[26] Leonid P. Pryadko and M.I. Dykman (unpublished).

[27] M. Abramowitz and I.A. Stegun, *Handbook of Mathematical Functions* (Dover, New York, 1970).

[28] A.F. Andreev, Zh. Éksp. Teor. Fiz. **78**, 2064 (1980) [Sov. Phys. JETP **51**, 1038 (1980)].

[29] M. Hruska and B. Spivak, Phys. Rev. B **65**, 033315 (2002).